Analysis of physical requirements for simple three-qubit and nine-qubit quantum error correction on quantum-dot and superconductor qubits

IlKwon Sohn, Seigo Tarucha, and Byung-Soo Choi

Phys. Rev. A **95**, 012306 — Published 6 January 2017

DOI: 10.1103/PhysRevA.95.012306

Analysis of Physical Requirement of Simple 3-qubit and 9-qubit QECs on Quantum-Dot and Superconductor Qubit

IlKwon Sohn[1],* Seigo Tarucha[2],† and Byung-Soo Choi[3‡]
[1]*School of Electrical Engineering, Korea University, Korea*
[2]*Department of Applied Physics, The University of Tokyo, Japan*
[3]*Electronics and Telecommunications Research Institute, Korea*

The implementation of a scalable quantum computer requires quantum error correction(QEC). An important step toward this goal is to demonstrate the effectiveness of quantum error correction where the fidelity of an encoded qubit is higher than that of the physical qubits. Therefore, it is important to know the conditions under which quantum error-correction code is effective. In this study, we analyze the simple three-qubit and nine-qubit quantum error-correction codes for quantum-dot and superconductor qubit implementations. First, we carefully analyze quantum error-correction codes and find the specific range of memory time to show the effectiveness of QEC and the best QEC cycle time. Second, we ran a detailed error simulation of the chosen error-correction codes in the amplitude damping channel, and confirmed that the simulation data agreed well with theoretically predicted accuracy and minimum QEC cycle-time. We also realize that since the SWAP gate worked fast on the quantum-dot qubit, it did not affect performance in terms of the spatial layout.

PACS numbers: 03.65.Wj, 03.67.Ac, 03.67.Lx

I. INTRODUCTION

The implementation of any practical quantum computer requires reliable building blocks formed by combining physical qubit devices with fault-tolerant quantum computation protocols [1, 2]. Of the many steps involved, the realization of an encoded qubit is the very first. In order to make a useful encoded qubit, we should choose an appropriate quantum error-correction code under the given physical capabilities such as the number of physical qubits and the fidelity of the physical gates. Following this, we need to show that the lifetime of the encoded qubit is longer than that of the physical qubit [3].

If the encoding succeeds in showing this gain, we say that the implementation is effective. Although many experiments have been undertaken in this vein, we still do not have a solid example of the effectiveness of quantum error correction(QEC) for arbitrary single error. Until now, the most advanced experiment of this sort has been conducted only to show repetitive bit-flip error correction under natural condition [4].

To show the effectiveness of the encoded qubit, it might be better to have a sufficient number of qubits and higher fidelity gates. However, it is difficult to determine whether such resources are sufficient without testing. Therefore, it is better to know the minimum conditions needed to exhibit effectiveness under the given quantum error-correction code as well as the minimum physical capability.

In this work, we consider the minimum conditions, especially the error rate of a physical qubit, that need to be satisfied to show the effectiveness of the quantum-dot and superconductor qubit technologies. Since these technologies face the difficulty of measurement and since only a small number of qubits have been realized thus far, we choose the simplest quantum error-correction codes, such as three-qubit [1, Ch. 10], [5, 6] and nine-qubit [7] without syndrome measurement. In this case, the data was encoded on a physical data qubit, and other physical qubits were used to check and correct the error.

In the first step, we analyze the three-qubit and nine-qubit quantum error-correction codes. Since our goal is to determine the maximal tolerable error rate of physical qubits, which depends on operation time, we define two times as T_{QEC} and T_{mem} for QEC protocol time and idle time between QEC cycles, respectively. Based on our analysis, we found that even if $T_{mem} = 0$, there is no gain in QEC since the QEC protocol adds more errors to the data qubit. We also found that the gain in QEC is only positive if $2T_{QEC} \leq T_{mem} \leq \frac{1}{2P_e}$, where P_e is the physical error rate during single-qubit gate operation time. From this, we realized that QEC should be conducted neither frequently nor rarely, and the best memory time is $T_{mem} = \frac{1-\sqrt{1-\frac{2}{3}(1+\frac{1}{9}P_e T_{QEC})}}{2P_e}$ in order to show maximum gain. Finally, the accuracy threshold value is $P_e = \frac{1}{3T_{QEC}}$. From the experimental point of view, this means that $T_2^\star$ should be three times T_{QEC} in units of single-gate operation time. Therefore, we can use this information as the precondition for the experimental effectiveness of QEC. Meanwhile this analysis gives an explanation for why many previous experiments were unable to show the effectiveness of QEC [5, 6, 8].

In the second step, we numerically analyze possible

* d2estiny@korea.ac.kr, First author
† tarucha@ap.t.u-tokyo.ac.jp
‡ bschoi3@etri.re.kr, First and Corresponding author

implementations of QEC on quantum-dot and superconductor qubit technologies. In order to implement the circuits, we compared the single-shot pulse and multiple-pulse methods. Due to the difficulty of finding a satisfactory single-shot pulse, we decided to use the multiple-pulse method. To reflect more practical situation, we applied the amplitude damping channel. Finally we confirmed that the numerical simulation yielded similar results to our theoretical analysis.

The reminder of this paper is organized as follows: Section II explains some preliminaries, whereas Section III describes the theoretical analysis of the circuits and their requirements for effectiveness. Section IV explains the numerical results under a practical situation which yielded similar results to the theoretical results. Section V discusses the verification of effectiveness in a the practical situation using the IBM Quantum Experience Section VI summarizes this work with a summary of avenues for future research.

II. PRELIMINARY

A. Error-Correction Codes

Following the first quantum error-correction code [7], many quantum error-correction codes have been proposed. More details as well as fault-tolerant implementation have been surveyed in [9–11]. Unfortunately, current device technologies cannot fully support many quantum error-correction codes. Therefore, it is better to consider the simplest quantum error-correction code at present. In this work, we choose the simplest quantum error-correction codes: the three-qubit QEC shown in Figure 1 and its generalization for the nine-qubit case shown in Figure 2.

The three-qubit code has been experimentally tested [5, 12]. This code can correct only a single type error such as the X error shown in Figure 1. It has four steps—encoding, free evolution (memory), decoding, and correction. For encoding, the target qubit information is located in the middle qubit, and two CNOT gates are used to entangle three qubits. Free evolution simply maintains the data qubit in its natural situation. During decoding, any single X error in the data qubit propagates to the two ancilla qubits. Note that any X error in the ancilla qubits cannot propagate to the data qubit. Therefore, only an X error on the data qubit has any effect. Finally, during the correction step, the possible X error can be corrected. No error can be corrected during the encoding, decoding, and correction steps. Moreover, it cannot correct a Z type error. Therefore, this simple code can correct a single X error during memory time.

In contrast to the three-qubit code, the nine-qubit code can correct any arbitrary single error in the data qubit. It is a concatenation code of two three-qubit codes for Z and X type error corrections consecutively. It can correct any single error during memory time. Since the necessary number of qubits is nine, the layout of the physical qubits and their interactions affect overall performance. As shown in Figure 2 we should add multiple SWAP gates for the 1D layout, whereas the 2D layout has no need of SWAP gates.

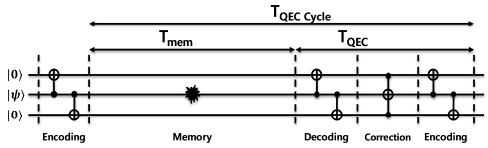

FIG. 1. Memory and QEC time for 3-qubit QEC.
This circuit was experimentally implemented in [5, 6]. A QEC cycle consists of Encoding, Memory, Decoding, and Correction steps. Ideally the QEC can correct a single X error in the data qubit during memory time. T_{mem}, T_{QEC}, and $T_{QEC\ Cycle}$ are times for memory, QEC, and the QEC cycle, respectively. Note that $T_{QEC\ Cycle}=T_{mem}+T_{QEC}$. To periodically operate this QEC circuit, each ancilla qubit should be reset at the end of the correction process which is omitted in the figure.

B. Effectiveness

Several recent experimental results have established that the feasibility of quantum error-correction codes [12, 13]. However, most results to this end have been obtained in artificial situations, such as applying the desired errors during memory time. A recent experimental result [4] has also shown the possibility of correcting the own error with the classical input state. Therefore, it remains challenging to determine whether the fidelity of the encoded qubit is higher than that of the physical qubit.

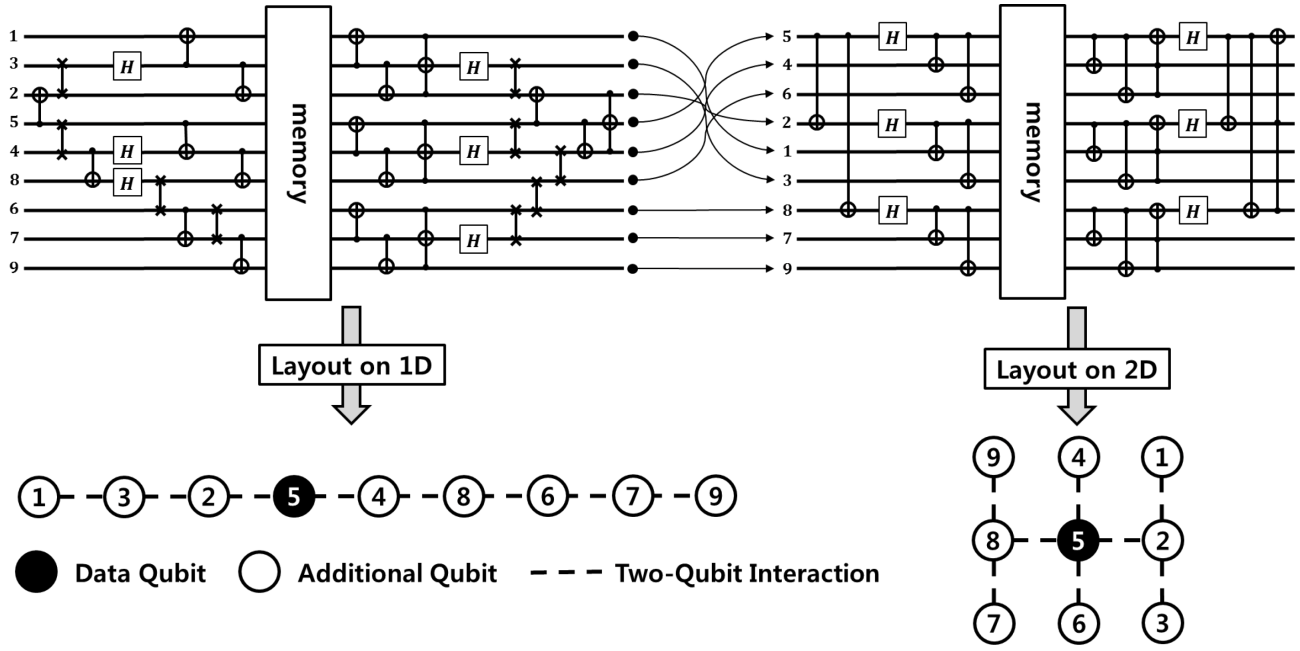

FIG. 2. Mapping of nine-qubit QEC on 1D and 2D architectures.
Due to the locality condition and the limit on the degree of interaction, multiple SWAP gates are augmented in the 1D architecture. The layout of the 1D structure was chosen such that it used few SWAP gates. After the last Toffoli gate, additional qubits (1∼4, 6∼9) should be reset and renamed like the beginning of the circuit.

If an implementation can show this property, we call it effective, and our goal is to analyze the minimal physical conditions for the simplest codes.

C. Error Models

Since we want to know the effectiveness of the code under a physical situation, we choose a dominant error model [14] for quantum dot physical qubits, as follows:

$$\Gamma_1 = \begin{pmatrix} 0 & \sqrt{\gamma_1 n_{th}} \\ \sqrt{\gamma_1(1+n_{th})} & 0 \end{pmatrix}, \tag{1}$$

$$\Gamma_2 = \begin{pmatrix} \sqrt{\gamma_2} & 0 \\ 0 & -\sqrt{\gamma_2} \end{pmatrix}, \tag{2}$$

where Γ_1 and Γ_2 are the relaxation and the dephasing operators. In these equations, γ_1 and γ_2 are the relaxation and dephasing rates of the qubit and, n_{th} is the bath temperature. For a single-qubit operation, there are two sources of errors: the error in the physical qubit, and the controlling error of the operation. However, we assume that single-qubit operation has the same error rate as the physical qubit for the necessary pulse time. Likewise, we assume that the two-qubit operation has the same error rate during pulse time. Note that since two-qubit operation involves two qubits, error in one qubit can propagate to the other qubit depending on the operation and type of error. To define the error rate, we use P_{e} as physical error rate on the physical qubit during π-pulse time of single-qubit operation. Therefore, although the physical time for two-qubit operation can be different from that for single-qubit operation, we use P_{e} for two-qubit operation as well.

D. Performance Measure

In this work, the fidelity of the encoded qubit is defined as the overlap of the density matrices of the data qubit and the ideal qubit. Since we also considered a numerical simulation, we use quantum process tomography [15] to obtain more precise information as follows.

$$F_{\mathrm{p}} = Tr(\chi_I \chi_{U_{data}}), \tag{3}$$

where χ_I is the process matrix [16] of the identity matrix, and $\chi_{U_{data}}$ is the process matrix of the data qubit following one round of the quantum error-correction cycle with different memory times.

III. THEORETICAL ANALYSIS

To know the physical requirements in order to render quantum error correction effective, we analyze the circuit itself. Since the strength of the error in the data qubit depends on memory time, we investigate the performance of the quantum error-correction code with variable memory time.

A. Analysis of Memory Time

1. Error Rate in terms of Time

In this work, we define P_{e} as the error rate of the physical qubit during single-qubit gate time. Based on this and the times for QEC and memory, we define two error rates as follows:

$$\begin{aligned} P_{\mathrm{QEC}} &= P_{\mathrm{e}} * T_{\mathrm{QEC}}, \\ P_{\mathrm{memory}} &= P_{\mathrm{e}} * T_{\mathrm{memory}}, \end{aligned} \tag{4}$$

where P_{QEC} and P_{memory} represent the error rate of the data qubit during QEC and memory, respectively. T_{QEC} is a constant with the physical implementation, but T_{memory} is variable.

2. Minimum Memory Time

We first consider the shortest memory time needed show effectiveness. To check the minimum memory time, we define two fidelities as follows.

$$\begin{aligned} F_{\mathrm{p}} &= 1 - P_{\mathrm{memory}} - P_{\mathrm{QEC}}, \\ F_{\mathrm{e}} &= 1 - \left[3P_{\mathrm{memory}}^2(1 - P_{\mathrm{memory}}) + P_{\mathrm{memory}}^3\right] \\ &\quad - \left[1 - (1 - P_{\mathrm{QEC}})^3\right] + \left[\frac{1}{9}P_{\mathrm{memory}}P_{\mathrm{QEC}}\right], \end{aligned} \tag{5}$$

where F_{p} and F_{e} represent the fidelities of the physical and the encoded qubits, respectively. The quantum error-correction codes are worth using when their circuits satisfy $F_{\mathrm{e}} \geq F_{\mathrm{p}}$. We assume that P_e reduces to 0 to derive a condition for $T_{\mathrm{memory,min}}$. It is not a lower bound or precise value but it can be used as a guideline to determine the minimum memory time. We can achieve the condition $T_{\mathrm{memory,min}} = 2T_{\mathrm{QEC}}$. This implies that if the memory time is too short—for example only one gate operation time—the quantum error-correction circuit cannot yield any effectiveness.

3. Maximum Memory Time

We also considered the duration for which memory time can show effectiveness. In this case, since $T_{\mathrm{QEC}} << T_{\mathrm{memory}}$, the two fidelities can be simplified as follows:

$$\begin{aligned} F_{\mathrm{p}} &= 1 - P_{\mathrm{memory}}, \\ F_{\mathrm{e}} &= 1 - \left[3P_{\mathrm{memory}}^2(1 - P_{\mathrm{memory}}) + P_{\mathrm{memory}}^3\right]. \end{aligned} \tag{6}$$

Again, to exhibit effectiveness, F_{e} should be greater than or equal to F_{p}. Based on this equation, we derive the as $P_{\mathrm{memory}} \leq \frac{1}{2}$, and hence $T_{\mathrm{memory,max}} \leq \frac{1}{2P_{\mathrm{e}}}$. This implies that we can delay error correction for sufficiently long. Meanwhile, if the time for the transversal gates is shorter than this memory time, we can apply multiple encoded operations instead of only one encoded gate between the QEC cycles. Note that this property has been recently investigated [17, 18].

4. Best Memory Time

We realize that there is a range of memory time to show effectiveness in, as $2T_{\mathrm{QEC}} \leq T_{\mathrm{memory,max}} \leq \frac{1}{2P_{\mathrm{e}}}$. Although we can choose any memory time within this range, it is better to choose one that shows the maximum gain, $F_e - F_p$, considering overhead due to error correction. From the above fidelities, we derive the best memory time as follows:

$$T_{\mathrm{memory,best}} = \frac{1 - \sqrt{1 - \frac{2}{3}(1 + \frac{1}{9}P_{\mathrm{e}}T_{\mathrm{QEC}})}}{2P_{\mathrm{e}}}. \tag{7}$$

5. Best QEC Cycle Time

Finally, we can set the best cycle time of QEC as follows.

$$\begin{aligned} T_{\mathrm{QEC\ Cycle}} &= T_{\mathrm{QEC}} + T_{\mathrm{memory,best}}, \\ &\simeq \frac{\sqrt{3} - 1}{2\sqrt{3}P_{\mathrm{e}}}, \\ &\simeq 0.211324\frac{1}{P_{\mathrm{e}}}, \end{aligned} \tag{8}$$

when $T_{\mathrm{QEC}} \ll 0$ is compared to T_{memory}. This condition implies that the best cycle time depends on the physical error rate. Therefore, we should set the appropriate cycle time depending on the physical error rate.

B. Accuracy Threshold Value

We define the maximum tolerable error rate as $1/T_{minimumcycletime}$ because if the encoded qubits are effective, their coherence time should be sustained for at least the length of the QEC cycle. Based on this definition, we can set the accuracy threshold value as follows:

$$\begin{aligned} P_{\mathrm{e,th}} &= \frac{1}{T_{\mathrm{QEC}} + T_{\mathrm{memory,min}}}, \\ &= \frac{1}{3T_{\mathrm{QEC}}}. \end{aligned} \tag{9}$$

This implies that the physical qubit should have $T_2^\star$ as $3T_{QEC}$. We summarize the above conditions in Table I.

TABLE I. Conditions

Parameter	Condition
$T_{\mathrm{memory,min}}$	$2T_{\mathrm{QEC}}$
$T_{\mathrm{memory,best}}$	$\frac{1-\sqrt{1-\frac{2}{3}(1+\frac{1}{9}P_{\mathrm{e}}T_{\mathrm{QEC}})}}{2P_{\mathrm{e}}}$
$T_{\mathrm{memory,max}}$	$\frac{1}{2P_{\mathrm{e}}}$
T_{QECCycle}	$0.211324\frac{1}{P_{\mathrm{e}}}$
$P_{\mathrm{e,th}}$	$\frac{1}{3}\frac{1}{T_{\mathrm{QEC}}}$

C. Explanation of Previous Experiment Results

In a previous experiment [6], the authors showed the possibility of correcting artificial errors. However, they were unable to show effectiveness. To explain their result, we applied the above conditions. Based on their design, $T_{\mathrm{QEC}} = 11/2$ was the single-qubit operation time unit. Therefore, by applying the above condition pertaining to the accuracy threshold value, $P_{\mathrm{e,th}}$ is 0.06. Unfortunately, the fidelity of the two-qubit gate, F_{CCZ}, in their work was 0.22, which was much higher than the threshold value. Therefore, their experiment cannot show effectiveness.

IV. NUMERICAL ANALYSIS

To check the above conditions and quantitatively analyze the physical design, we numerically investigated the actual situation by using an error simulation.

A. Pulse Sequence

To check the physical situation, we should decompose the given quantum error-correction circuit into the form of a physical pulse sequence that can be tailored to the target qubit system. As the simplest approach, it was possible to use a single-shot pulse for the entire circuit. On the contrary, we could have used a general method, such as concatenating the predefined pulse sequence for each elementary gate, which we call the multiple pulse method. To determine which approach was better, we investigated two CNOT and Toffoli gates.

Using the multiple pulse method, we were able to decompose the CNOT gate into the several pulses for the quantum-dot [21, 22] and superconductor [6, 23] qubits, as shown in Figure 3. The Toffoli gate was also decomposable as shown in Figure 4.

For the single-shot pulse method, we used the GRAPE method [24], which attempts to find a better by using the numerical approach. As an example, Figure 5 shows a single-shot pulse sequence for the CNOT gate on the quantum-dot qubit. Since the performance of the generated pulse sequence depends on many configuration, it is generally difficult to find a good single-shot pulse sequence.

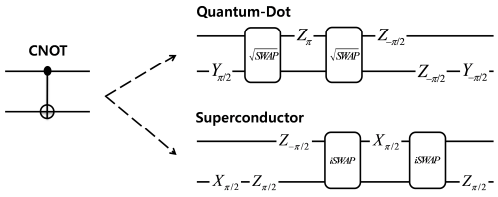

FIG. 3. CNOT Gate by Multiple Pulses.
Each qubit technology supports arbitrary single-qubit gates. For two-qubit gate, quantum-dot[19] and superconductor[20] qubits support $SWAP(\theta)$ and $iSWAP(\theta)$ interactions, respectively.

Finally, we compared the two approaches by checking the process fidelity with the error rate. As shown in Tables II and III, the multiple pulse method exhibited the best performance in the range of small error rate. Therefore, we subsequently choose the multiple pulse method.

B. Performance Analysis

Finally, we numerically simulated the quantum error-correction circuit under the amplitude damping channel model with different error rates. Figure 6 shows the gain in quantum error-correction code with different memory times and error rates. From this figure, we see that if the time for memory is too small, there is no gain. We also confirmed that a satisfactory range of memory time depends on error rate.

We calculated the physical time of needed for implementation as well as the necessary conditions, such as minimum memory time and accuracy threshold values,

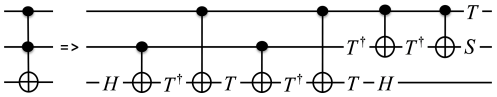

FIG. 4. Toffoli Gate by Multiple Pulses.[1].

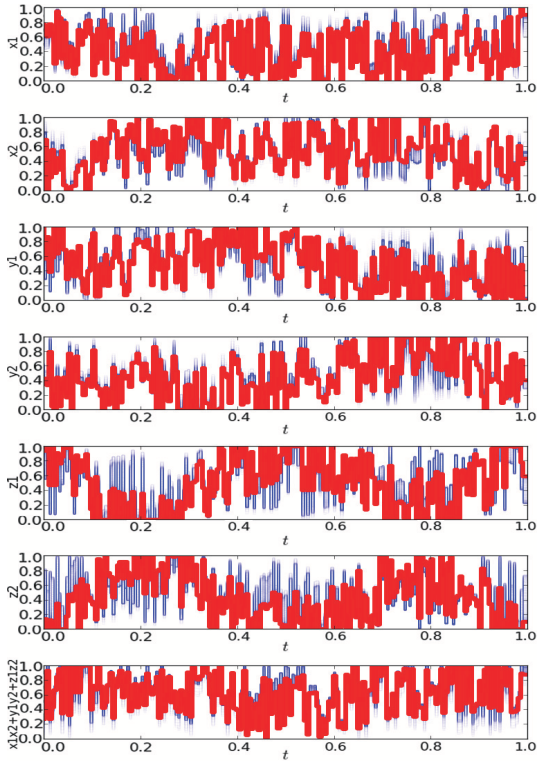

FIG. 5. CNOT Gate by Single-Shot Pulse.
Each figure shows the pulse waveform for x_1, x_2, y_1, y_2, z_1, z_2, and $x_1x_2 + y_1y_2 + z_1z_2$ Hamiltonians, respectively. The horizontal line represents the time of pulse sequence during unit time. The red(thin) curves show the final pulse shape, and the blue(thick) curves for intermediate pulse shapes during pulse generation.

as shown in Table IV. Two key parameters, the accuracy threshold value and the minimum memory time, are marked in Figure 6. As shown in the figure, our theoretical analysis agreed well with the results of the numerical simulation.

C. Impact of Architectures

Since the simple three-qubit code cannot support arbitrary single-qubit error, it is reasonable to consider the nine-qubit code, which can correct any arbitrary single-qubit error. In this case, we should consider the impact of the physical layout of qubits, such as 1D or 2D. Since the nine-qubit code requires multiple non-neighbor qubits, it is necessary to find an appropriate mapping to a 2D structure, which requires the use of several SWAP gates. Therefore, the performance of the SWAP gate might affect overall performance. Tables V and VI show the time for the quantum error-correction circuit and its accuracy threshold value for different layouts. For the quantum-dot qubit, since the SWAP gate operated quickly, there was not a significant difference.

V. IBM QUANTUM EXPERIENCE TEST

To check whether our theoretical analysis fit actual quantum hardware, we used IBM Quantum Experience[25]. IBM Quantum Experience provides a five-qubit superconductor quantum processor for users online.

A. Correctness Analysis

To show the correctness of QEC, we considered artificial errors in the data qubit. Artificial errors are not natural, such as decoherence during memory time, but errors inserted as gates without memory time. We used the same QEC circuit as in Figure 1, but in IBM superconductor qubits, only the third qubit can be used for a target qubit of a CNOT gate. Moreover it does not support a Toffoli gate. We changed the circuit to the one shown in Figure 7.

We checked the fidelity of the data qubit with the artificial errors. We also considered both bit-flip and phase-flip errors to check the dominant error type. Table VII shows the fidelities of the data qubit after the correction of each error type. Since fidelity was close to one,

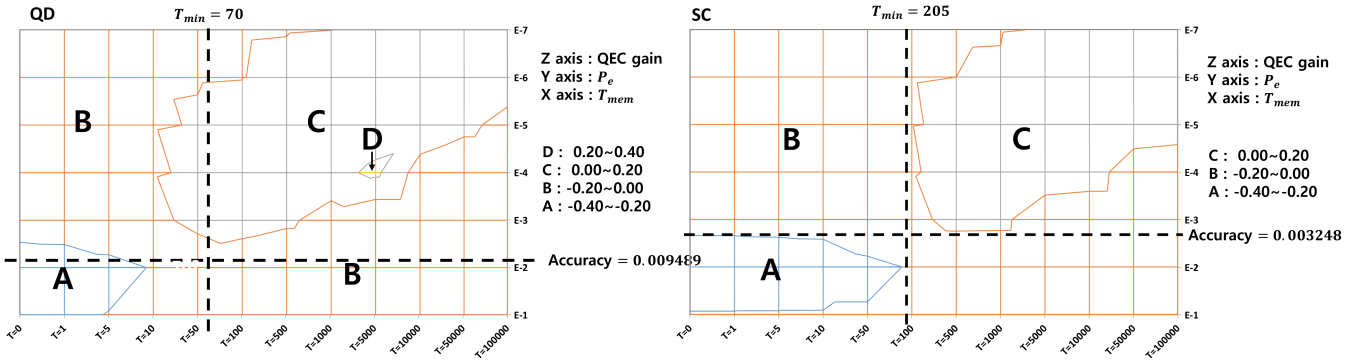

FIG. 6. (color online) Gain of 3-qubit QEC with memory time and physical error rate.
The range in green represents memory time and physical error rate, showing positive gain($F_e - F_p$) of QEC. The dotted lines represent the theoretically calculated minimum memory time and accuracy threshold value shown in Table IV.

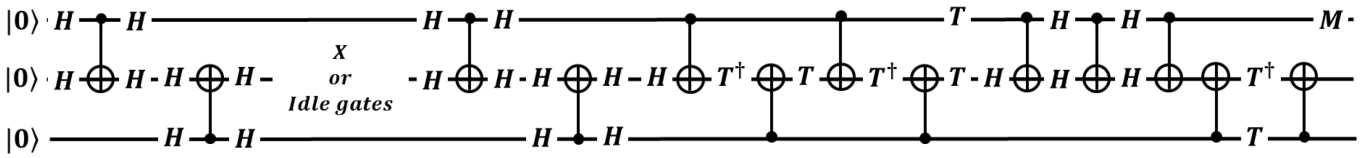

FIG. 7. Converted circuit of 3-qubit QEC for IBM test with an intended error and idle gates. The second qubit in this figure was the third input to the IBM system.

TABLE II. Error Tolerance of the CNOT Gate.
Each column and row represents a different relaxation and dephasing rate, respectively. Since the pulse sequence was approximate, fidelity was not one, even though relaxation and dephasing were zero.

(a) Single-Shot Pulse				
	0.00000	0.00001	0.00010	0.00100
0.00000	0.99793	0.99789	0.99753	0.99394
0.00001	0.99791	0.99787	0.99751	0.99392
0.00010	0.99773	0.99769	0.99733	0.99375
0.00100	0.99593	0.99859	0.99594	0.99196
(b) Multiple Pulses				
	0.00000	0.00001	0.00010	0.00100
0.00000	0.99999	0.99989	0.99897	0.98984
0.00001	0.99979	0.99968	0.99877	0.98964
0.00010	0.99795	0.99785	0.99693	0.98783
0.00100	0.97985	0.97975	0.97885	0.96992

TABLE III. Error Tolerance of the Toffoli Gate.
Each column and row represents a different relaxation and dephasing rate, respectively.

(a) Single-Shot Pulse				
	0.00000	0.00001	0.00010	0.00100
0.00000	0.59219	0.59215	0.59185	0.58877
0.00001	0.59217	0.59214	0.59185	0.58875
0.00010	0.59202	0.59198	0.59167	0.58860
0.00100	0.59047	0.59043	0.59012	0.58706
(b) Multiple Pulses				
	0.00000	0.00001	0.00010	0.00100
0.00000	0.99970	0.99858	0.98842	0.89298
0.00001	0.99743	0.99631	0.98617	0.89096
0.00010	0.97727	0.97617	0.96625	0.87300
0.00100	0.80014	0.79925	0.79115	0.71518

TABLE IV. Key Parameters

	Quantum-Dot	Superconductor
T_{QEC}	$\frac{281}{8}$	$\frac{821}{8}$
$P_{\mathrm{e,th}}$	0.009489	0.003248
$T_{\mathrm{memory,min}}$	$\simeq 70$	$\simeq 205$

we confirmed that the circuit could correct correctable error.

B. Effectiveness Analysis

As stated above, we wanted to find when the encoded qubit yields better performance than the physical qubit. Thus, we inserted several IDLE gates to prolong memory time to check effectiveness in a the practical situation. Unfortunately, the IBM device does not support a sufficient number of steps to minimize memory time. It allowed for only 40 steps, and the converted circuit had 31 steps. According to the result in Section III, the minimum memory time should be $2T_{QEC}$ steps, which here

TABLE V. T_{QEC} with 1D and 2D Architectures

T_{QEC}	Equation	QD	SC
1D(QD)	5 T_{SWAP}+8T_{CNOT}+2T_{Toffoli}	$\frac{672}{8}$	▪
1D(SC)	6 T_{SWAP}+7T_{CNOT}+2T_{Toffoli}	▪	$\frac{2220}{8}$
2D	8 T_{CNOT}+2T_{Toffoli}	$\frac{562}{8}$	$\frac{1642}{8}$

TABLE VI. $P_{\mathrm{e,th}}$ with 1D and 2D Architectures

$P_{\mathrm{e,th}}$	QD	SC
1D	0.0039682	0.0012012
2D	0.0047449	0.0016240

meant 62 steps. Therefore, we were unable to check the minimum memory time. However, we could test a memory time over nine-idle gates, although it was not helpful. Table VIII shows the degradation in the data qubits with a small number of steps for memory time. With this circuit, we checked that the three-qubit QEC did not show any effectiveness using fidelities from the test. Table VIII shows the results of the test. This results can be considered to show that the theoretical analysis of minimum memory time was correct, but we could not check the QEC gain of the real hardware in maximum and best memory times.

VI. CONCLUSION AND FUTURE WORKS

In this work, we investigated the physical condition that needed to be satisfied to meet the requirements for the effectiveness of quantum error-correction code. For the quantum-dot and superconductor qubits and their current and near future capabilities, we considered the simplest three-qubit quantum error-correction code with a coherent correction method. We first analyzed the circuit and found that there is a range of memory time that exhibits the effectiveness of the code. Note that even if memory time is zero, it cannot exhibit effectiveness. To confirm this, we conducted an error simulation using the amplitude damping channel. The simulation confirmed that there is a range of memory time with a different physical error rate. We also investigated the impact of layout, such as 1D or 2D on the nine-qubit code. In the case where the performance of the SWAP gate is good, we found the difference in physical layout does not affect performance.

Since the current study considers only the encoded memory qubit, it can be used for any application which requires only the memory capability such as the quantum repeater node [26]. Since the quantum repeater node requires the longer memory time for longer distance, the above analysis can be used to find the tradeoff between the best number of hops without doing quantum error-correction. Also we can consider the decoding and the implementation of entanglement swapping protocol at the physical level with purification protocol.

TABLE VII. Fidelities of 3-qubit QEC with intended errors

Fidelity	F_p
Bit flip code	0.765
Phase flip code	0.783

TABLE VIII. Fidelities of 3-qubit QEC with insufficient number of idle gates

Fidelity	F_p	F_e
Bit flip code	0.984	0.852
Phase flip code	0.973	0.860

ACKNOWLEDGMENTS

We are grateful to Robert Johansson and Rodney Van Meter. This work was supported by Electronics and Telecommunications Research Institute (ETRI) grant funded by the Korean government. [16ZH1100, Research and Development of Quantum Computing Platform and its Cost-Effectiveness Improvement]. This work was supported by the MSIP(Ministry of Science, ICT and Future Planning), Korea, under the ITRC(Information Technology Research Center) support program (IITP-2015-R0992-15-1017) supervised by the IITP(Institute for Information & communications Technology Promotion). This work was supported by CREST, JST, ImPACT Program of Council for Science, Technology and Innovation (Cabinet Office, Government of Japan), and JSPS, Grant-in-Aid for Scientific Research S (No. 26220710).

[1] M. A. Nielsen and I. L. Chuang, *Quantum Computation and Quantum Information* (Cambridge University Press, 2000).

[2] R. Van Meter and C. Horsman, Commun. ACM **56**, 84 (2013), URL `http://doi.acm.org/10.1145/2494568`.

[3] The lifetime of each qubit is based on the gate operation time. In the encoded qubit case, the non-transversal gates may consume multiple gate operation time so we consider the gate operation time based on the transversal gates.

[4] J. Kelly, R. Barends, A. G. Fowler, . A. Megrant, E. Jeffrey, T. C. White, D. Sank, . J. Y. Mutus, B. Campbell, Y. Chen, et al., Nature **519**, 66 (2015), URL `http://dx.doi.org/10.1038/nature14270`.

[5] P. Schindler, J. T. Barreiro, T. Monz, V. Nebendahl, D. Nigg, M. Chwalla, M. Hennrich, and R. Blatt, Science **332**, 1059 (2011).

[6] M. D. Reed, L. DiCarlo, S. E. Nigg, L. Sun, L. Frunzio, S. M. Girvin, and R. J. Schoelkopf, Nature **482**, 382 (2012), URL http://dx.doi.org/10.1038/nature10786.

[7] P. W. Shor, Phys. Rev. A **52**, R2493 (1995).

[8] D. Nigg, M. Mller, E. A. Martinez, P. Schindler, M. Hennrich, T. Monz, M. A. Martin-Delgado, and R. Blatt, Science **345**, 302 (2014).

[9] D. Gottesman (2009), http://arxiv.org/abs/0904.2557, URL http://arxiv.org/abs/0904.2557.

[10] S. J. Devitt, K. Nemoto, and W. J. Munro (2009), http://arxiv.org/abs/0905.2794, URL http://arxiv.org/abs/0905.2794.

[11] B. M. Terhal (2013), http://arxiv.org/abs/1302.3428, URL http://arxiv.org/abs/1302.3428.

[12] D. G. Cory, M. D. Price, W. Maas, E. Knill, R. Laflamme, W. H. Zurek, T. F. Havel, and S. S. Somaroo, Phys. Rev. Lett. **81**, 2152 (1998), URL http://link.aps.org/doi/10.1103/PhysRevLett.81.2152.

[13] X.-C. Yao, T.-X. Wang, H.-Z. Chen, W.-B. Gao, A. G. Fowler, R. Raussendorf, Z.-B. Chen, N.-L. Liu, C.-Y. Lu, Y.-J. Deng, et al., Nature **482**, 489 (2012).

[14] Christoph Kloeffel, and Daniel Loss, Annu.Rev.Conden.Ma.P. **4**, 51-81 (2013), URL http://annualreviews.org/doi/10.1146/annurev-conmatphys-030212-184248.

[15] A. Gilchrist, N. K. Langford, and M. A. Nielsen, Phys. Rev. A **71**, 062310 (2005), URL http://link.aps.org/doi/10.1103/PhysRevA.71.062310.

[16] A. G. White, A. Gilchrist, G. J. Pryde, J. L. O'Brien, M. J. Bremner, and N. K. Langford, J. Opt. Soc. Am. B **24**, 172 (2007).

[17] Y. S. Weinstein, Phys. Rev. A **88**, 012325 (2013), URL http://link.aps.org/doi/10.1103/PhysRevA.88.012325.

[18] Y. S. Weinstein, Phys. Rev. A **89**, 020301 (2014), URL http://link.aps.org/doi/10.1103/PhysRevA.89.020301.

[19] Colin P. Williams, *Explorations in Quantum Computing* (Springer, 2011).

[20] Norbert Schuch, and Jens Siewert, Phys. Rev. A **67**, 032301 (2003), URL http://link.aps.org/doi/10.1103/PhysRevA.67.032301.

[21] D. Loss and D. P. DiVincenzo, Phys. Rev. A **57**, 120 (1998), URL http://link.aps.org/doi/10.1103/PhysRevA.57.120.

[22] R. Brunner, Y.-S. Shin, T. Obata, M. Pioro-Ladrière, T. Kubo, K. Yoshida, T. Taniyama, Y. Tokura, and S. Tarucha, Phys. Rev. Lett. **107**, 146801 (2011), URL http://link.aps.org/doi/10.1103/PhysRevLett.107.146801.

[23] J. M. Chow, Ph.D. thesis (2010).

[24] B. Rowland and J. A. Jones, Philosophical Transactions of the Royal Society A: Mathematical, Physical and Engineering Sciences **370**, 4636 (2012).

[25] IBM Quantum Experience, URL http://www.research.ibm.com/quantum

[26] W. Dür, H.-J. Briegel, J. I. Cirac, and P. Zoller, Phys. Rev. A **59**, 169 (1999).